**BEST: International Journal of Management Information Technology and Engineering (BEST: IJMITE)**
**ISSN (P): 2348–0513, ISSN (E): 2454–471X**
**Vol.11, Issue 1, Jun 2023, 27–42**


# A REVIEW OF NOVEL TECHNIQUES FOR SWITCHED RELUCTANCE MACHINE TO REDUCE TORQUE RIPPLE

**DEEPA NIDANAKAVI[1], Dr. KRISHNAVENI.K[2] & Dr. MALLESHAM.G[3]**

[1]Department of Electrical Engineering, Osmania University, Hyderabad, India

[2]Department of Electrical and Electronics Engineering, CBIT, Hyderabad, India

[3]Department of Electrical Engineering, Osmania University, Hyderabad, India

## ABSTRACT

Electric motors are crucial parts for a wide range of applications, but there are numerous choices. Without the expensive cost or torque ripple issues of induction or permanent magnet motors, for instance, inverter frequency machines offer tremendous power and reliability. Notwithstanding the benefits over other electric motors that SRM offers, its biggest disadvantage is that it needs a more complicated control system. Commutation switching machines have downsides, especially when operating at high speeds, such as acoustic noise and torque ripple. Which system will benefit from the low torque ripple and acoustic noise varies frequently on the application being utilized, thus it is difficult to say. We examine these common tendencies in technology and how they aid in reducing machine noise and torque ripple.

**Keywords:** Switched Reluctance Drive (SRD), Torque Ripple (TR), Current Ripple (CR), Torque Sharing Function(TSF), Direct Instantaneous Torque Function(DITC), Rotorangle, Highspeed, Effienciency.

## 1. INTRODUCTION

Switched reluctance motors (SRMs) have a robust mechanical design and are distinguished by their simple construction. The motor structure consists of a steel stator and rotor. On the stator's poles, the windings are evenly spaced out.. The simplicity of these structures makes them an attractive choice for a variety of applications from household appliances to automotive and heavy industrial applications. [1-3]. Absence of permanent magnet devices makes SRM a promising alternative to permanent magnet motors as permanent magnets are expensive. Variable rate applications of adaptive SRM have proven slow in research over the past 20 years [4] despite the inherent robustness of SRMS despite its simplicity and extensive development capabilities.

Especially when placed in a servo type application the control requirements that the SRM has to meet can be complicated. These leaks may not be hazardous to your system in all cases but according to the application being torsion waveforms and resulting acoustic noise are hazardous to your system. Compared to other round core AC motors the SRM offers relatively high torque ripple due to its structure as a double boss single excitation motor and non-linear magnetic properties in light of the non-linear inductance profile of the SRM. . 56]. Torque ripple is negligible in a servo or servo system. In these systems the presence of torque ripple is strongly felt by the user or can be simulated unsafely under load and watches have overcome this problem with practical success over the last decade. Considerable progress has been made and it is now evident that drives built Large torque waves in the early phases of growth are exceedingly loud [7].SRM applications can be improved by reducing torque ripple. This can be achieved mainly in two ways. One approach is to

enhance the machine's design. in terms of magnetic design and the other is to apply modern electronic control techniques. Torque pulsation can be limited by changing the structure of the poles of the stator and rotor. But these changes come at the expense of producing specific engines for SRM. Approaches to adjusting the control parameters in the electronic control unit such as the current level supply voltage and the changes of the on and off angles which affect the electromagnetic torque generated in the SRM which in turn depends on the excitation angle which corresponds to the position eats the Electronic control approaches to minimize rotor torque ripple can reduce the average torque output. This is due to the lack of full use of the engine characteristics at all power levels. [8] Some other methods include applying sense coil to detect phase finite element method (FEM). This document features a review. of torque ripple minimization techniques using SRM. The document is formatted in the following order: Section II presents the basic details of the anything like the mechanical structure of the SRM and approaches to torque generation. Section III discusses the operating conditions that lead to torque ripple. Section IV reviews the achievement of optimization of the control method and machine design to reduce torque ripple.

## 2. Switched Reluctance Motor Structure

The stator, rotor, and winding are the three components that make up the SRM's structure. Figure 1 [19] depicts the most popular classic SRMs with stator and rotor pole ratios. The internal flux is discovered to have the least amount of resistance. And the electromagnetic torque in the SRM is brought on by this tendency. The highest inductance of the excited phase is reached when the rotor pole and stator pole are lined up.

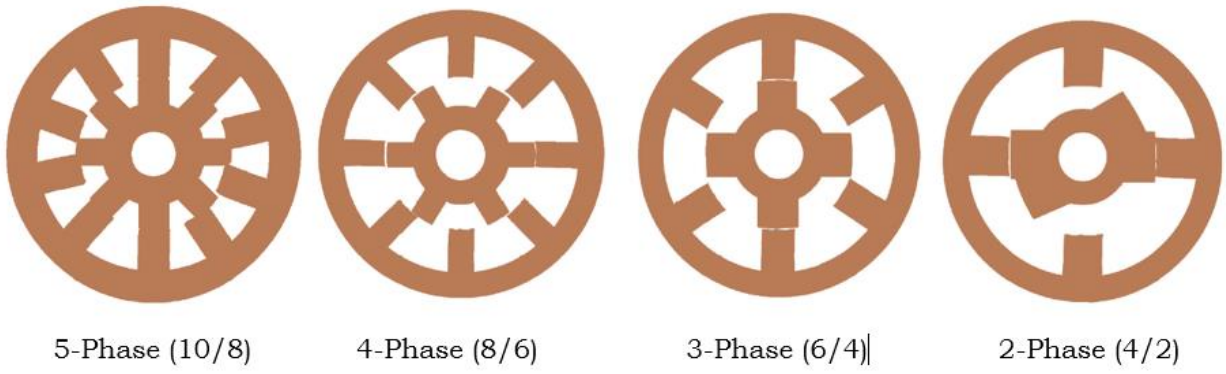


**Figure 1.**SRM Structure

$V=iR+d\theta/dt$

Can be used to represent the equation for the instantaneous voltage between two phase terminals.

Where I is the phase current, R is the resistance of a phase, V is the instantaneous voltage across each phase, t is the time, is the flux linkage, and I is the phase current. Flux linkage variation depending on the phase current value and the rotor position

$$V = iR + \frac{\partial \phi}{\partial I}\frac{dj}{dt} + \frac{\partial \phi}{\partial \theta}\frac{dx}{dt}$$

$$= iR + M(\theta, j)\frac{dj}{dt} + E(\theta, j)\frac{dx}{dt}$$

E(θ,j) is the reverse electromotive force (EMF), M(θ,J) is the instantaneous inductance, and is the rotor's position.

It is expected that the SRM's mechanical equation is [10]

$$J\frac{dg}{dt} = T1_e - T1_L - T1_0$$

$$\omega = \frac{dx}{dt}$$

In this equation, J is the rotational inertia, is the rotation's angular speed, T1 e is the electromagnetic moment, T1 L is the load moment, and T1 0 is the extra moment, which includes the frictional moment, air-torque resistance, and other moments. The authors of [11] presented an enhanced 12/8 pole SRM for electric vehicles and hybrid electric vehicles (HEV). Torque ripple is decreased by 10.2% and average torque is raised by 2.4% using this optimisation technique.These values are expressed relative to a typical reference design. Thus, in [11], the authors concluded that the initial torque can most effectively be increased by increasing the diameter of the rotor.

**1.1. Winding Configurations**

The winding configuration governs the SRMS performance. In Figure 2, descriptions of winding configurations for different reluctance motors are given [1214]. Wrapping the phase windings across one pole of the stator by placing one coil in each track is a configuration known as a single layer focus winding (SLC). The other configuration is a single layer coil (SLMC) and a mutually coupled SLC coil with separate winding directions. The induced change in inductance and mutual induces torque in the SRM for the SLMC coil. And the transformation of the inductor itself generates the torque in the conventional SRM for the SLC coil [1516]. In another mutually coupled dual layer coil (DLMC) configuration, each slot is shared by two coils. The same is done in a dual-layer concentrator coil (DLC). Figure 3 shows the representation of the DLMC and DLC configurations. And another coil configuration is the Full Pitch (FP) coil configuration shown in Figure 4. Here, coupled SRM (MCSRM), a distributed winding SRM, is utilised. The use of SLMC and DLC may not be possible for particular polar and stator phase combinations.

Windings that are out of balance is one of the causes..

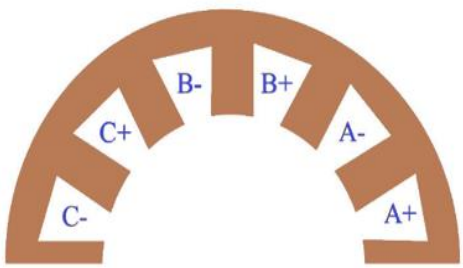


SLC

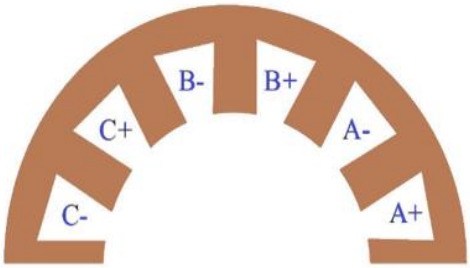


SLMC

**Figure 2:**single-layer concentrated (SLC) winding and single-layer mutually coupled (SLMC) windings.

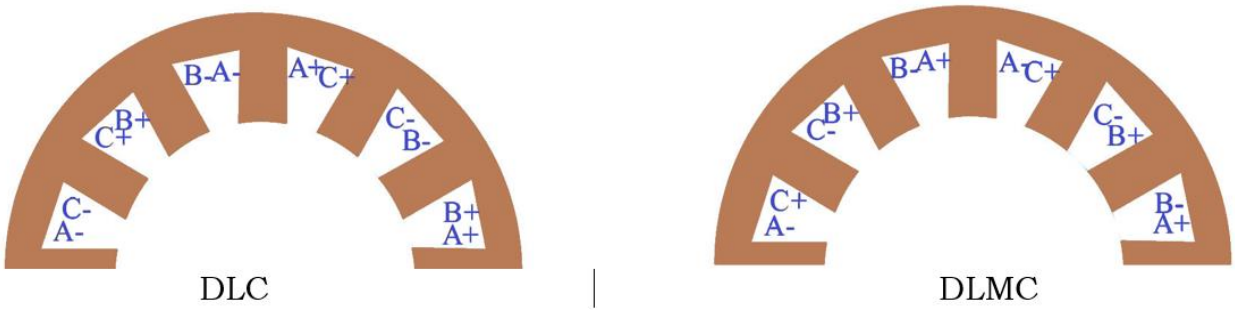


**Figure 3:** double-layer concentrated (DLC) winding and double-layer mutually coupled (DLMC) windings.

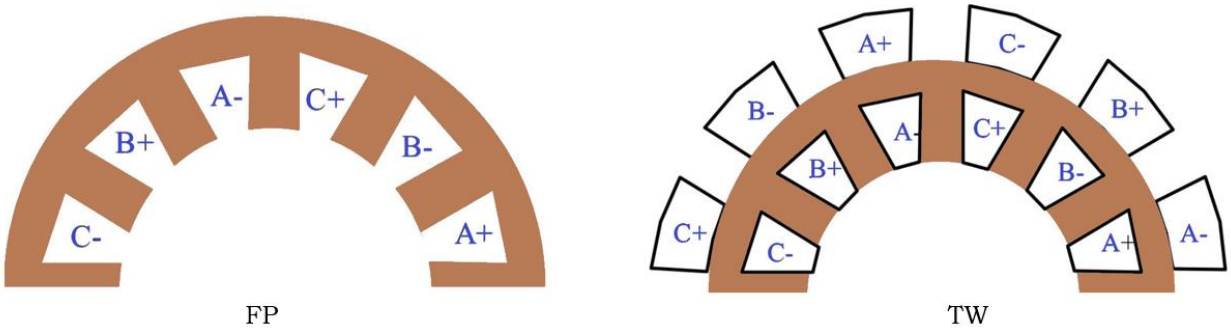


**Figure 4:** fully-pitched (FP) and toroidal winding.

To lower eddy and hysteresis current losses, a special multilayer isolated flux SRM (MIFPS) has been suggested [17&18]. A more torque-dense arrangement than a conventional SRM is what distinguishes this one. Fig. 4 also displays the toroidal coil arrangement. With 12/10 MIFP and SRM, she uses. Due to the possibility of making the teeth of the stator and rotor wide, the toroidal winding enhances heat transfer, which is advantageous. With a higher fill factor and consequently lower acoustic noise at low speeds, the MCSRM configuration produces more torque per amp performance. Moreover, at faster speeds than in the MCSRM [19&20], the backEMF voltage is higher. Lower torque ripple and average power are preferred when comparing the coil designs mentioned above. 1.1. Calculation of torque in a switching reluctance motor. The fundamental principle of electromechanical energy conversion in solenoid coils explains the generation of torque in SRM.

In Figure 5(a), a revolving solenoid N is shown. The current i, excites the electromagnetic coil and produces a magnetic flux $\phi$. With the increase in excitation current, the armature moves towards the fixed yoke the excitation current's magnetic force acting under its influence [25].

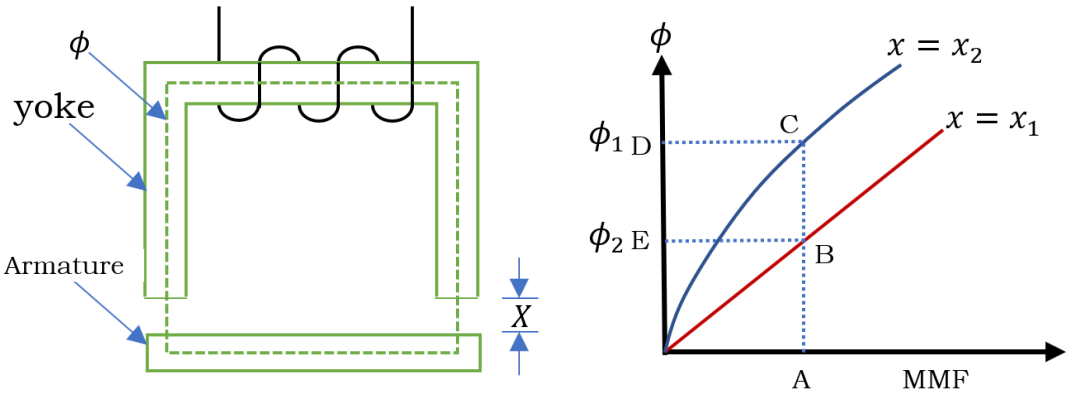


**Figure 5:** Solenoid and its characteristics. (a) A solenoid. (b) Flux v. mmf characteristics.

A graph of flux and magnetic force (mm) for two different air gap values, x 1 and x 2, is shown in Figure 5(b). It is decided that x 1>x 2 for the clearances x 1 and x 2. According to the graph, the clearing reluctance is more prevalent and the flux characteristics for x 1 are linear when compared to mmf, which results in a weaker flux in the magnetic circuit. [25] gives the input of electrical energy

$$.W_e = \int ei\, dt = \int i\, dt \frac{dN\phi}{dt} = \int Ni\, d\phi = \int F\, d\phi$$

where F is the mmf and e is the induced emf. The total energy stored in the coil, W f, is equal to this input electrical energy, W e, and the energy that was successfully transmitted mechanically, W m, is written. $W_e = W_f + W_m$

When the mechanical work is zero, like when the armature starts at position x 1, the electrical energy input and the stored field energy are equal. This matches the OBEO region depicted in Figure 5. (b). The area of the OBAO, as illustrated in Figure 5(b), provides the complement of the field energy, known as co-energy, which can be expressed mathematically as dF. Similar to this, at the x 2 position of the armature, the co-energy is provided by the OCAO area, and the field energy is correlated with the OCDO area. For incremental modifications, $\delta W_e = \delta W_f + \delta W_m$

The following energies are inferred for the continuous excitation of F1 caused by operating point A in Figure 5(b): $\delta W_e = \int_{\phi_1}^{\phi_2} F_1 d\phi = F_1(\phi_2 - \phi_1) = \text{area(BCDEB)}$

$$\delta W_f = \delta W_{f|_{x=x_1}} - \delta W_{f|_{x=x_2}} = \text{area(OCDO)} - \text{area(OBEO)}$$

Then,

$$\delta W_m = \delta W_e - \delta W_f = \text{area(OBCO)}$$

and for a given magnetic force, it is the region created between two curves. When a rotating machine is involved, the additional mechanical energy represented in terms of electromagnetic torque and the shift in the rotor position is provided by: $\delta W_n = T_e \delta\theta$

Where T_e is the electromagnetic torque and δθ is the increasing rotor angle. So the electromagnetic torque is given by

$$T_{el} = \frac{\delta W_g}{\delta\theta}$$

The additional mechanical effort required is equal to the rate of change of the co-energy, which is nothing more than the addition of the field energy, when the excitation condition is constant (i.e., when constant MMF is taken into account). So, [26] expresses the extra mechanical work as follows: $\delta W_k = \delta W_g'$

$$W_g' = \int \phi \, dF = \int \phi \, d(Nj) = \int (N\phi) \, dj = \int \lambda(\theta, j) dj = \int L(\theta, j) j \, dj$$

where the rotor position and current are functions of the inductance, L, and the magnetic flux connections,. A co-energy change happens when two rotor locations, _2 and _1, are taken into account. As a result, the clearance torque is shown as a function of rotor position and current using the formula

$$T_{el} = \frac{\delta mg}{\delta\theta} = \frac{\delta W_k'}{\delta\theta} = \left.\frac{\delta W_k'(j, \theta)}{\delta\theta}\right|_{i=constant}$$

The torque can be calculated as follows for a given current assuming the inductance changes linearly with the position of the rotor, which turns out to be common but is not the case in practise.

$$T_{el} = \frac{dL(\theta, j)}{d\theta} \frac{j^2}{2}$$

Where

$$\frac{dL(\theta, j)}{d\theta} = \left.\frac{L(\theta_2, j) - L(\theta_1, j)}{\theta_2 - \theta_1}\right|_{i=constant}$$

And this differential inductance can be thought of as aNmA2, which is the torque constant.

The electromagnetic torque produced is proportional to the square of the current, as shown in the equations above, and a unipolar current is required to produce a DC torque. Also, this requirement for a unipolar current is favorable in terms of the switching circuit's need for a power switch. The motor is connected to the converter circuit's output. To regulate the current in the phase coil [27] of the SRM, only one power switch is needed. The switching circuit requires significantly fewer power switches as a result of this functionality. The drive is more cost-effective as a result of the converter's reduced switching power. The torque's characteristic is related to the square ofA controllable converter is required for the SRM. It cannot work directly on three-phase power lines. This property results in a relatively expensive motor drive compared to induction and synchronous motors, when used for constant speed applications. The reliance on the power converter makes it a variable-speed motor drive system in essence [28]. The clearance torque can be adjusted accurately by the current control. The clearance torque is inversely related to the excitation current or

current fluctuation in various machines, including AC and DC machines [29]. As a result, the torque control is located inside the machine itself. And as a result, the system now transforms into a linear torque amplifier, allowing the drivetrain to manage speed at extremely high speeds. In the SRM, the connection between the clearance torque and excitation current is nonlinear. Three non-linear routes in SRM are influenced by the three-way relationship between the magnetic flux linkages, the rotor position, and the excitation current.

Relationship in dimensions between excitation current, rotor position, and clearance torque. It is possible to generate the excitation current reference from the gap torque reference.

## 3. RESULTS

Two minimization techniques are approaches are there in minimization of torque ripples [32].

- Machine Design Improvement
- Control Strategy Improvement

### 3.1. Torque Ripple Minimization Through Machine Design

Torque ripple is minimised in SRM by machine design and magnetic design, with the design processes described in [33] taking torque ripple and acoustic noise generation during the design process into consideration. The stator and rotor pole shapes, as well as the machine's properties (torque, speed, noise, etc.), are defined by mathematical calculations. The stator arc, Bs, rotor arc, and are the variables that influence torque ripple., which are determined for the design of the machine. To minimize torque ripple and generated noise, the magnetic behavior can be determined using Finite Element Analysis (FFA) tools and in the design [34] including The inclination of the rotor pole is shown. The main purpose of the rotor construction is to weaken torque ripple while maintaining a high torque density. With this design, there is no development in torque density, but shows a development in torque ripple factor and the disadvantage is that it can lead to extreme torque dissipation. The maximum is achieved due to the increased effective clearances due to the new geometric design of the rotor/stator poles.

### 3.2. Torque Ripple Minimization Through Control Strategy Improvements

#### A. Current Profiling

The shaping of the current is known as current profiling. The immediate value of the current and the inductance determine the torque that is generated. Consequently, torque ripple can be reduced via current profiling. By structuring the current using the phase current profiling process, torque ripple is reduced. Using the three-dimensional connection, the excitation current reference is derived from the air gap torque reference. Several academic works suggested numerous modern profiling techniques. The control algorithm used in the implementation varies between the suggested ways in these literatures most of the time [35]. The main idea behind current profiling is to model the controller to follow the generated current after enumerating the current's shape using an offline technique to achieve zero torque ripples.. Based on the rotor position step and current machine specifications, the current profile is then generated. The maximum and minimum currents are calculated as follows [40]:

$$i_{max}(\theta_K) = j(\theta_{K-1}) + \frac{1}{L\left(j(\theta_{K-1}, \theta_{K-1})\right)}\left(v - iR(\theta_{K-1}) - \frac{dL(j(\theta_{K-1}), \theta_{K-1})}{d\theta}\omega j(\theta_{K-1})\right)dt$$

$$i_{min}(\theta_K) = j(\theta_{K-1}) + \frac{1}{L(j(\theta_{K-1}, \theta_{K-1}))}\left(-v - iR(\theta_{K-1}) - \frac{dL(j(\theta_{K-1}), \theta_{K-1})}{d\theta}\omega j(\theta_{K-1})\right)dt$$

The new current profile boundaries are determined as $i_{max}$ and $i_{min}$.

The relationship of $I = f(T, \theta)$ is then computed using a current profiling control algorithm. The torque ripple is found to Curtail up to 18 % by the current profiling method [41].

**Torque Sharing Function**

The torque sharing function is important to the current profiling method because it involves a single shape and is often used in torque ripple mitigation engineering. Torque is shaped by further measuring the position of the rotor angle [42]. To meet the primary objective of low torque ripple, TSFs are provided for ideal torque sharing between individual phases. TSF is based on commonly used linear, sine, exponential and cubic curves, and TSF curves are used to represent the TSF that determines the SRM and the demand for torque ripple [43]. The Torque Sharing Function (TSF) intelligently divides the reference constant torque between specific phases by defining a reference current profile for each phase. Ideally, when this current reference configuration is monitored by a current controller, the total torque contribution from all phases adds up to a constant torque, eliminating torque ripple. twisted. A very simple way to define the torque sharing function is to use analytic expressions to model the dynamic behavior of the phase torquecontribution [44].

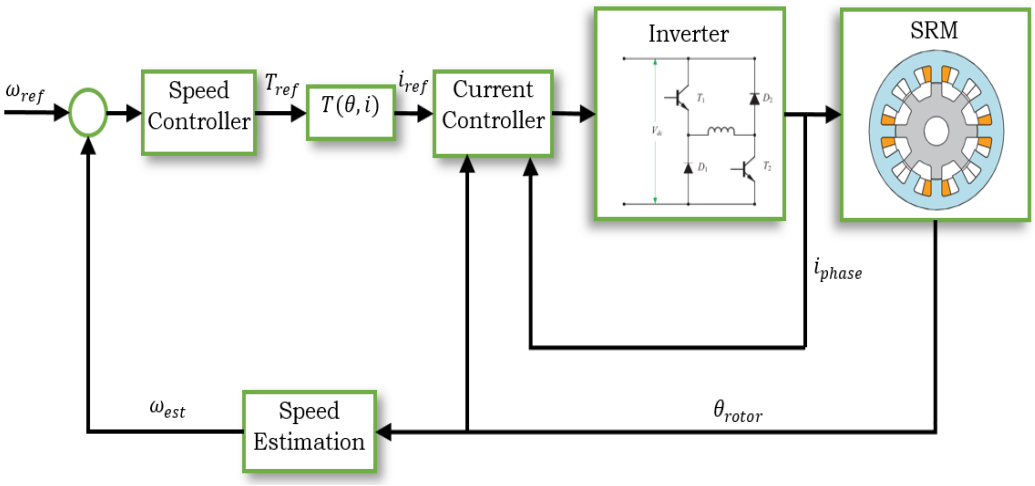


**Figure 6:** Overview of control structure for SRM with TSF.

the torque reference of the $i^{th}$ phase is defined as [45]

$$T_{ref}(i) = \begin{cases} 0 & 0 \le \theta < \theta_{ON} \\ T_{ref} f_{rise}(\theta)\theta_{ON} \le \theta < \theta_{ON} + \theta_{OV} \\ T_{ref}\theta_{ON} + \theta_{OV} \le \theta < \theta_{OFF} \\ T_{ref} f_{fall}(\theta)\theta_{OFF} \le \theta < \theta_{OFF} + \theta_{OV} \\ 0 & \theta_{OFF} + \theta_{OV} \le \theta < \theta_p \end{cases}$$

where T_ref(i) is the reference torque for the i-th phase, T_ref is the total reference torque, f_rise(θ) is the gain function for the incident phase increasing from 0 to 1, and f_fall(θ) is the function decrease for the go period. phase decreases from one to zero, for a given position of the rotor,

### B. Direct Instantaneous Torque Control

A high-precision rotor position sensor is not necessary with the direct instantaneous torque control (DITC), a controlledtechnique that was presented in 2003. The switching waveform, the current or torque waveforms, or the instantaneous torque values are not employed in DITC. based on SMR terminal measurement. To accurately simulate the phase current as a function of torque and rotor position, a complicated model is needed. [46].

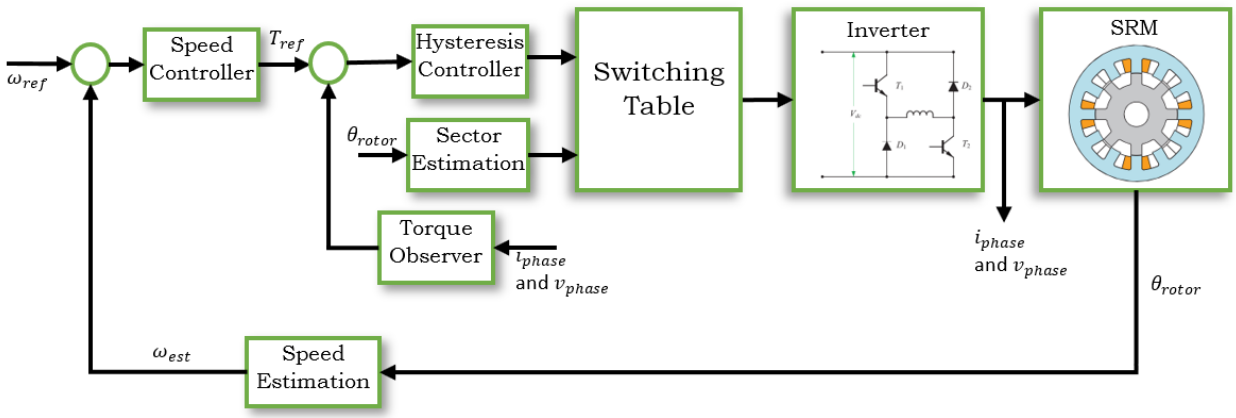


**Figure 7:** DITC control system block diagram.

As torque T(,i) depends on current and rotor position, good rotor position measurement is necessary for both accurate torque calculation and accurate control. Instead of being a function of the avoided rotor position T(,i), the torque characteristic is a function of flux linkage. The total torque T tot is calculated using a lookup table. A digital torque hysteresis controller and switching signals are used to generate all of the machine's active stages [47].

Hysteretic controllers need a wide range of operation in order to provide high-bandwidth switching signals. By employing DITC to condense the torque pulsations that contribute to torque ripple, the torque ripple is reduced to the absolute minimum. The torque ripple drops to 38% of the machine's typical torque of 40N-m after one simulation

## 4. Review of Previous Work

In [49], a non-dominant sort genetic algorithm (NSGA11) for SRM optimization is presented and a gap length is proposed for SMR. Maximum efficiency, maximum average torque and minimum iron weight are realized in a multi-purpose design. Finite element analysis (FEA) was used to obtain values during optimization, and 8/6, 6/4 SRM designs were implemented. Design parameters improve average torque and efficiency with reduced iron weight.

In [50], Jaya Multi-objective method is used to optimize the SRM design where the diversity is higher as shown in the results and 8/6.6/4 is optimized by the algorithm. MoJAYA. The results of MoJAYA were compared with the Non-Dominant Sort Genetic Algorithm (NSGA11). The software FEMM4.2 is used in the optimization program in the Lua programming language.

In [51] to optimize the structural design of the 12/8 switching reluctance motor is used by a single-target genetic algorithm. Optimizing output torque by narrowing each tooth root out of the four tooth roots, enlarging each tooth root out of the four tooth heads and increasing the stator outside diameter is the main goal of this optimization to Optimized output torque. Here, a small electric car using a 12/8 switching reluctance motor and finite elements is used to evaluate the motor model. The upgraded engine provides a 25% increase in average torque compared to the original design.

In [52], an ant colony optimization approach was used to find the best engine design parameters for ISRM. Optimize torque and efficiency by setting optimization parameters to motor dimensions. MATLAB software is used to determine the torque and efficiency coefficients by considering the motor's nonlinearity in the analytical model. In [53], this paper uses a corresponding nonlinear torque model, which is Recursively Resistant Quadratic Support Vector Regression (RR-LSSVR). Segment motors are modeled as SR motors (SSRM) and feature nonlinear characteristics of magnetic field and torque. This particular algorithm has been proven to be fast and accurate, as well as an accurate inductance measurement method and torque calculation procedure. Compared to other models, RR-LSSVR corrects the weights based on errors, improves the accuracy of the model under real-world conditions built with 16/10 SSRM, and recommends it. [54] In electric vehicles (EVs), SRM is optimized using a 3-phase 12/8 Gray Wolf Optimizer (GWO) and increases the SRM output torque density. The proposed engine characterization and optimization procedure was performed using the FEM approach. Optimization constraints detail current density, optimization procedure, maximum flux density, and other motor sizes. Optimized values are sent to the FEM software for analysis for each iteration to obtain optimal values. Simultaneously built working prototype engine and exterior can be tested empirically. The torque can be increased by 120% while keeping the method the same volume.

In [55] two types of uncertainty like variation outer disorder and the model error are in traditional H-infinity control which has an external control method. The H-infinity control mechanism is a closed loop controller, decisive the ideal control weight is difficult. The ideal weight for the transfer function matrix is suggested control process by an effective optimization tool and Genetic algorithm (GA) is used. By this technique, the SRMS speed is adjusted using MATLABS built-in toolset and in each interval the weight noise setting is resolute. H-infinity optimum control use GA method to get the ideal weight noise setting.

In [56] This research provides a unique multi objective optimization design technique for a switching reluctance motor (SRM) for low-speed electric cars and the design parameters for SRM are acceleration time, maximum speed, maximum climbing gradient, torque ripple factor, and energy usage ratio to optimized the SRMs performance. By using the MATLAB/Simulink, the SRMS finite element model and the vehicle balance equation, a dynamic simulation model for a low-speed pure EV propulsion system was created. The geometric parameters of the SRM are then optimized for many objectives by using Taguchi-Chicken swarm optimization technique.

In [57] Switching frequency drives (SRM) are an excellent support option for variable speed operation. The linear quadratic regulator using Process Integrated (LOI) technology is flexible and easy to change when the plant is used in state

space and manual adjustment of the Q and R matrix weights is provided by the LQR system and It can be accomplished. your needs. A field experiment and evaluation between descriptive algorithms for the design of LQI controllers and PID controllers is performed to determine the best approach for modifying the LQI controller design of Q and R variables in SR engines. In this work the LQI parameters are weighted in an optimal way and the gain of the controller can be repeatedly adjusted which makes the hybrid controller (LQI GA) more efficient in controlling the multivariate system.

In [58] The hybrid electric vehicles (HEVs) are cost-effective to increase the vehicle's reliability and lower its fuel usage by using the belt-driven starter/generator (BSG) and decrease CO2 emission to 10%. Motor and generator are served by the core of the BGS system in an electrical unit and proved the novel multimode optimization technique for switching reluctance machines in order to optimize the motor and generator simultaneously. The multi objective optimization takes seven different design factors and four different driving modes. Sum of techniques is used to rise the efficiency of multimode optimization. The Kriging model is used to approximate the FEM throughout the optimization process and optimum designs increase the SSRMS presentation in all operating conditions.

| Method | Implemented Process | Merits | Demerits | Ref |
|---|---|---|---|---|
| SPAM (Angle Modulation) | Find the on and off angles, determine the required current amplitude and phase angles | Better efficiency, improved torque/speed ratio, reduced ripples in the torque | Controlling torque and current mutually is no possible, storage of huge current data increases the cost | 59 |
| DTC and ATC | Estimation of torque during speed control and torque control using hysteresis bands | Rapid torque control by DTC, torque ripple minimization to IEEE standards | Parameters of the machine should be known | 60 |
| Torque sharing function -based method | Torque sharing function, generating current refence using torque control, using hysteresis band to track reference current | Easy torque control, torque waveform determination, smooth torque over a wide speed range | Need iTθ characteristic, desired torque waveform | 61 |
| **Table 1: Cont** | | | | |
| Feedback linearization control | Converting a non-linear system into a linear model | Reduced torque ripple, no non-linear terms in the feedback loop, providing the necessary decoupling between currents | Does not adapt to changes of uncertain parameters, complex algorithms | 62 |
| Iterative learning controller | Add offset current to phase current reference to monitor current | No need to define system parameters, achieve perfect current monitoring under different operating conditions | Transient degradation performance, limited iteration cycle | 63 |
| Intelligent control | Used for offline or online phase current optimization | Powerful self-learning, adaptability, reduce torque ripple, independent of machine parameters, | Complicated calculation algorithm | 64 |
| Share conversion | Split-ended single-ended half-bridge converter. | Minimize the number of electrical appliances | The fault tolerance will be reduced, the current stress in the switch and the common diode is higher | 65 |
| Split | Midpoint voltage comp | Motor efficiency is increased | effect of medium | 66 |

| | | | | |
|---|---|---|---|---|
| converters | ensation method | with reduced midpoint voltage fluctuations. | voltage oscillation and poor fault tolerance | |
| Cdump converter | Cdump converter with inductor | faster degaussing during phase replacement, energy after discharge to capacitor, used directly in next phase and not back to DC power | need extra capacitor and switch current pressure is high | 67 |
| FS-PTC | enhanced torque control aware of binding state | limit the increase in torque of the drive motor exchanger reluctance (SRM) | affect the reader's ability. Total disk space reduced by 4-9% | 68 |

One of the most important techniques for reducing SRM torque ripple is called TSF-DITC, which is based on the torque sharing function (TSF) and direct instantaneous torque control (DITC). In this method, the entire torque is divided among the phases using the TSF, and the phases' torque hysteresis then drives the motor in accordance with the necessary control rule. In Reference [69], a multi-stage converter is shown. It is decided to use a multi-level translator based on TSF-DITC, and various control rules are chosen for various operator domains. This quickens the station's excitation and demagnetization processes, enabling faster torque tracking. [70] proposes an optimal angle adaption TSF-based direct instantaneous torque control technique for SRM. Reference [71] enhances the system using a dynamic amorphous TSF.

## 5. CONCLUSIONS

This is a significant disadvantage of using SRM torque ripple commercially. In industrial applications, torque ripple, which increases vibration and noise, could not be a useful feature of SRMs. For SRMs working in commercial applications, reducing SRM torque ripple is crucial. By enhancing the mechanical design described in this study, torque ripple can be decreased. Reduced torque oscillations brought on by mechanical design flaws also result in increased mechanical complexity, higher production costs, and a reduction in the maximum torque. A torque ripple counter measurement that is more cost-effective and ideal is made possible by controlling torque ripple. The various control strategies to lessen torque ripple were examined and modified in this work. Every method put out makes the torque ripple brought on by SRM worse.There are still instances where SRMs operate to such a degree that torque ripple is not fully taken into account, despite significant attempts to reduce torque ripple. A number of useful functions for switching reluctance motor modelling, design analysis, and control have undergone a complete revision. Switched reluctance motors have seen scientific advancement, yet there still seems to be a big gap in terms of industrial applications. By creating inexpensive controllers that set standards and can be used in motion control systems, current research trends aim to close this gap.

## REFERENCES

1. Lopez, Gabriel Gallegos. Sensorless control for switched reluctance motor drives. University of Glasgow (United Kingdom), 1998.
2. Sirimanna, Samith, et al. "Comparison of electrified aircraft propulsion drive systems with different electric motor topologies." Journal of Propulsion and Power 37.5 (2021): 733-747.
3. Mvungi, Nerey H. "Sensorless commutation control of switched reluctance motor." World Academy of Science, Engineering and Technology 25 (2007): 325-330.
4. Donaghy-Spargo, C. M. "Synchronous reluctance motor technology: opportunities, challenges and future direction." Engineering & technology reference. (2016): 1-15.
5. Mitra, Rakesh, and Yilmaz Sozer. "Torque ripple minimization of switched reluctance motors through speed signal processing." 2014 IEEE Energy Conversion Congress and Exposition (ECCE). IEEE, 2014.

6. Tseng, K. J., and Shuyu Cao. "A SRM variable speed drive with torque ripple minimization control." APEC 2001. Sixteenth Annual IEEE Applied Power Electronics Conference and Exposition (Cat. No. 01CH37181). Vol. 2. IEEE, 2001.
7. Chuang, Tzu-Shien. "Acoustic noise reduction of a 6/4 SRM drive based on third harmonic real power cancellation and mutual coupling flux enhancement." Energy Conversion and Management 51.3 (2010): 546-552.
8. Chai, J. Y., Y. W. Lin, and C. M. Liaw. "Comparative study of switching controls in vibration and acoustic noise reductions for switched reluctance motor." IEE Proceedings-Electric Power Applications 153.3 (2006): 348-360.
9. Kazemi, A. R., et al. "A novel sensorless method for rotor position detection in bifilar SRM drive." 2010 IEEE International Conference on Power and Energy. IEEE, 2010.
10. Zhang, Man, et al. "Improvement of the variable turn-off angle control for SRM regarding vibration reduction." 2017 IEEE International Electric Machines and Drives Conference (IEMDC). IEEE, 2017.
11. Ding, Wen, et al. "Design consideration and evaluation of a 12/8 high-torque modular-stator hybrid excitation switched reluctance machine for EV applications." IEEE Transactions on industrial electronics 64.12 (2017): 9221-9232.
12. Mousavi-Aghdam, Seyed Reza, et al. "Design and analysis of a novel high-torque stator-segmented SRM." IEEE Transactions on Industrial Electronics 63.3 (2015): 1458-1466.
13. Asgar, Majid, EbrahimAfjei, and Hossein Torkaman. "A new strategy for design and analysis of a double-stator switched reluctance motor: Electromagnetics, FEM, and experiment." IEEE Transactions on Magnetics 51.12 (2015): 1-8.
14. Li, G. J., et al. "Comparative study of switched reluctance motors performances for two current distributions and excitation modes." 2009 35th Annual Conference of IEEE Industrial Electronics. IEEE, 2009.
15. Ma, X. Y., et al. "Recent development of reluctance machines with different winding configurations, excitation methods, and machine structures." CES Transactions on Electrical Machines and Systems 2.1 (2018): 82-92.
16. Ma, X. Y., et al. "Quantitative analysis of contribution of air-gap field harmonics to torque production in three-phase 12-slot/8-pole doubly salient synchronous reluctance machines." IEEE Transactions on Magnetics 54.9 (2018): 1-11.
17. Burress, Tim, and Curt Ayers. "Development and experimental characterization of a multiple isolated flux path reluctance machine." 2012 IEEE Energy Conversion Congress and Exposition (ECCE). IEEE, 2012.
18. AndradaGascón, Pedro. "SRM drives an alternative for E-traction: Presentation of the workshop." Workshop SRM Drives an Alternative for E-Traction: Proceedings: February 2, 2018, EPSEVG-UPC Vilanovai la Geltrú (Barcelona) Spain. UniversitatPolitècnica de Catalunya. GAECE-Grupd'AccionamentsElèctricsambCommutacióElectrònica, 2018.
19. Kabir, MdAshfanoor, and Iqbal Husain. "Design of mutually coupled switched reluctance motors (MCSRMs) for extended speed applications using 3-phase standard inverters." IEEE Transactions on Energy Conversion 31.2 (2015): 436-445.
20. Li, G. J., et al. "Comparative studies of torque performance improvement for different doubly salient synchronous reluctance machines by current harmonic injection." IEEE Transactions on Energy Conversion 34.2 (2018): 1094-1104.
21. Azer, Peter, Berker Bilgin, and Ali Emadi. "Comprehensive analysis and optimized control of torque ripple and power factor in a three-phase mutually coupled switched reluctance motor with sinusoidal current excitation." IEEE Transactions on Power Electronics 36.6 (2020): 7150-7164.
22. Ma, Xiyun, et al. "Investigation on synchronous reluctance machines with different rotor topologies and winding configurations." IET Electric Power Applications 12.1 (2018): 45-53.
23. Dong, Jianning, et al. "Advanced dynamic modeling of three-phase mutually coupled switched reluctance machine." IEEE Transactions on Energy Conversion 33.1 (2017): 146-154.
24. Reddy, Battu Prakash, Prathap Reddy Bhimireddy, and SivakumarKeerthipati. "A sense winding system and dynamic current profiling to reduce torque ripple of SRM." International Transactions on Electrical Energy Systems 30.2 (2020): e12261.
25. Meng, Bin, et al. "Novel magnetic circuit topology of linear force motor for high energy utilization of permanent magnet: Analytical modelling and experiment." Actuators. Vol. 10. No. 2. MDPI, 2021.
26. Ling, Xiao, et al. "Precise in-situ characterization and cross-validation of the electromagnetic properties of a switched reluctance motor." Artificial Intelligence in Agriculture 4 (2020): 74-80.
27. Sovicka, Pavel, PavolRafajdus, and Vladimir Vavrus. "Switched reluctance motor drive with low-speed performance improvement." Electrical Engineering 102.1 (2020): 27-41.
28. Riyadi, Slamet. "A control strategy for SRM drive to produce higher torque and reduce switching losses." Journal of Electrical Systems 14.4 (2018): 205-216.
29. Khan, Yawer Abbas, and VimleshVerma. "Novel speed estimation technique for vector-controlled switched reluctance motor drive." IET Electric Power Applications 13.8 (2019): 1193-1203.
30. Ma, Mingyao, et al. "A switched reluctance motor torque ripple reduction strategy with deadbeat current

control." 2019 14th IEEE Conference on Industrial Electronics and Applications (ICIEA). IEEE, 2019.
31. Kumagai, Takahiro, Jun-ichi Itoh, and Keisuke Kusaka. "Reduction method of torque ripple, dc current ripple, and radial force ripple with control flexibility of five-phase srm." 2020 IEEE Energy Conversion Congress and Exposition (ECCE). IEEE, 2020.
32. MoradiCheshmehBeigi, Hassan, and AlirezaMohamadi. "Torque ripple minimization in SRM based on advanced torque sharing function modified by genetic algorithm combined with fuzzy PSO." International Journal of Industrial Electronics Control and Optimization 1.1 (2018): 71-80.
33. Lee, Jin Woo, et al. "New rotor shape design for minimum torque ripple of SRM using FEM." IEEE transactions on magnetics 40.2 (2004): 754-757.
34. Kabir, MdAshfanoor, and Iqbal Husain. "Segmented rotor design of concentrated wound switched reluctance motor (SRM) for torque ripple minimization." 2016 IEEE Energy Conversion Congress and Exposition (ECCE). IEEE, 2016.
35. Dúbravka, Peter, et al. "Control of switched reluctance motor by current profiling under normal and open phase operating condition." IET Electric Power Applications 11.4 (2017): 548-556.
36. Khalili, H., E. Afjei, and A. Najafi. "Torque ripple minimization in SRM drives using phase/current profiles." 2007 International Aegean Conference on Electrical Machines and Power Electronics. IEEE, 2007.
37. Mitra, Rakesh, et al. "Torque ripple minimization of switched reluctance motors using speed signal based phase current profiling." 2013 IEEE Energytech. IEEE, 2013.
38. Saidani, Sihem, Mohamed RadhouanHachicha, and MoezGhariani. "A New Phase Current Profiling with FLC for Torque Optimization of 12/8 SRM." International Journal of Electrical & Computer Engineering (2088-8708) 6.5 (2016).
39. Mikail, Rajib, et al. "Four-quadrant torque ripple minimization of switched reluctance machine through current profiling with mitigation of rotor eccentricity problem and sensor errors." IEEE Transactions on Industry Applications 51.3 (2014): 2097-2104.
40. Huang, Liren, et al. "Novel current profile of switched reluctance machines for torque density enhancement in low-speed applications." IEEE Transactions on industrial electronics 67.11 (2019): 9623-9634.
41. Makino, H., et al. "Instantaneous current profiling control for minimizing torque ripple in switched reluctance servo motor." 2015 IEEE Energy Conversion Congress and Exposition (ECCE). IEEE, 2015.
42. Xue, X. D., Ka Wai Eric Cheng, and Siu Lau Ho. "A control scheme of torque ripple minimization for SRM drives based on flux linkage controller and torque sharing function." 2006 2nd international conference on power electronics systems and applications. IEEE, 2006.
43. Chithrabhanu, Arun, and Krishna Vasudevan. "Online compensation for torque ripple reduction in SRM drives." 2017 IEEE Transportation Electrification Conference (ITEC-India). IEEE, 2017.
44. Li, Haoding, Berker Bilgin, and Ali Emadi. "An improved torque sharing function for torque ripple reduction in switched reluctance machines." IEEE Transactions on Power Electronics 34.2 (2018): 1635-1644.
45. Xia, Zekun, et al. "A new torque sharing function method for switched reluctance machines with lower current tracking error." IEEE Transactions on Industrial Electronics 68.11 (2020): 10612-10622.
46. Sun, Jianzhong, et al. "Simulation of the direct instantaneous torque control of SRM using MATLAB." International Conference on Automatic Control and Artificial Intelligence (ACAI 2012). IET, 2012.
47. Xu, Aide, et al. "A new control method based on DTC and MPC to reduce torque ripple in SRM." IEEE Access 7 (2019): 68584-68593.
48. Veena, Nayak D., and Naik L. Raghuram. "Minimization of torque ripple using DITC with optimum bandwidth and switching frequency for SRM employed in electric vehicle." 2017 International Conference on Smart grids, Power and Advanced Control Engineering (ICSPACE). IEEE, 2017.
49. El-Nemr, Mohamed, et al. "Finite element based overall optimization of switched reluctance motor using multi-objective genetic algorithm (NSGA-II)." Mathematics 9.5 (2021): 576.
50. Afifi, Mohamed, et al. "Multi-Objective Optimization of Switched Reluctance Machine Design Using Jaya Algorithm (MO-Jaya)." Mathematics 9.10 (2021): 1107.
51. Sholahuddin, Umar, AgusPurwadi, and YanuarsyahHaroen. "Structural Optimizations of a 12/8 Switched Reluctance Motor using a Genetic Algorithm." International Journal of Sustainable Transportation Technology 1.1 (2018): 30-34.
52. YILDIZ, Ahmet, Mehmet POLAT, and MahmutTemelÖzdemir. "Design optimization of inverted switched reluctance motor using ant colony optimization algorithm." 2018 International Conference on Artificial Intelligence and Data Processing (IDAP). IEEE, 2018.
53. Wu, Jiangling, Xiaodong Sun, and Jianguo Zhu. "Accurate torque modeling with PSO-based recursive robust LSSVR for a segmented-rotor switched reluctance motor." CES Transactions on Electrical Machines and Systems 4.2 (2020): 96-104.
54. Vuddanti, Sandeep, Vinod Karknalli, and Surender Reddy Salkuti. "Design and comparative analysis of three phase, four phase and six phase switched reluctance motor topologies for electrical vehicle propulsion." Bulletin

of Electrical Engineering and Informatics 10.3 (2021): 1495-1504.
55. Rigatos, Gerasimos, PierluigiSiano, and SulAdemi. "Nonlinear H-infinity control for switched reluctance machines." Nonlinear Engineering 9.1 (2020): 14-27.
56. Hajiabadi, Hojjat, Mohsen Farshad, and MohammadAliShamsinejad. "Multi-objective optimization and online control of switched reluctance generator for wind power application." International Journal of Industrial Electronics Control and Optimization 4.1 (2021): 33-45.
57. Souza, Darielson A., et al. "Optimal lqi and pid synthesis for speed control of switched reluctance motor using metaheuristic techniques." International Journal of Control, Automation and Systems 19.1 (2021): 221-229.
58. Bai, Shengxi, and Chunhua Liu. "Overview of energy harvesting and emission reduction technologies in hybrid electric vehicles." Renewable and Sustainable Energy Reviews 147 (2021): 111188.
59. Gundogmus, Omer, et al. "Current profile optimization method for simultaneous dc-link current ripple and acoustic noise minimization in switched reluctance machines." 2020 IEEE Energy Conversion Congress and Exposition (ECCE). IEEE, 2020.
60. Sun, Xiaodong, et al. "Direct torque control based on a fast modeling method for a segmented-rotor switched reluctance motor in HEV application." IEEE Journal of Emerging and Selected Topics in Power Electronics 9.1 (2019): 232-241.
61. Üstün, Oğuz, and MithatÖnder. "An improved torque sharing function to minimize torque ripple and increase average torque for switched reluctance motor drives." Electric Power Components and Systems 48.6-7 (2020): 667-681.
62. Bober, Peter, and ŽelmíraFerková. "Comparison of an off-line optimized firing angle modulation and torque sharing functions for switched reluctance motor control." Energies 13.10 (2020): 2435.
63. Shao, Zhen, and Zhengrong Xiang. "Adaptive iterative learning control for switched nonlinear continuous-time systems." International Journal of Systems Science 50.5 (2019): 1028-1038.
64. Kumar, R. Senthil, et al. "Intelligent Fuzzy controller based NT control of 5Φ SRM." Materials Today: Proceedings (2021).
65. Hu, Yanfang, Tao Wang, and Wen Ding. "Performance evaluation on a novel power converter with minimum number of switches for a six-phase switched reluctance motor." IEEE Transactions on Industrial Electronics 66.3 (2018): 1693-1702.
66. Y. Hu, C. Gan, W. Cao, C. Li and S. J. Finney, "Split Converter-Fed SRM Drive for Flexible Charging in EV/HEV Applications," in IEEE Transactions on Industrial Electronics, vol. 62, no. 10, pp. 6085-6095, Oct. 2015, doi: 10.1109/TIE.2015.2426142.
67. Setiawan, Kho Lukas Budi. "Analysis Performance of Capacitor Voltage in C-Dump Converter for SRM Drive." 2018 IEEE Student Conference on Research and Development (SCOReD). IEEE, 2018.
68. Li, Cunhe, et al. "An improved finite-state predictive torque control for switched reluctance motor drive." IET Electric Power Applications 12.1 (2018): 144-151.
69. Yang, Yang, et al. "Torque Compensation Method of Switched Reluctance Motor Adopting MPC Based on TSF-DITC." Progress In Electromagnetics Research M 110 (2022): 211-221.
70. Ren, Ping, et al. "Minimization of torque ripple in switched reluctance motor based on MPC and TSF." IEEJ Transactions on Electrical and Electronic Engineering 16.11 (2021): 1535-1543.
71. Sun, Xiaodong, et al. "Torque ripple reduction of SRM drive using improved direct torque control with sliding mode controller and observer." IEEE Transactions on Industrial Electronics 68.10 (2020): 9334-9345.